Hindawi Publishing Corporation
Journal of Nanomaterials
Volume 2012, Article ID 930763, 5 pages
doi:10.1155/2012/930763

Research Article

Characterization of Orthorhombic α-MoO_3 Microplates Produced by a Microwave Plasma Process

Arrak Klinbumrung,[1] Titipun Thongtem,[2,3] and Somchai Thongtem[1,3]

[1] *Department of Physics and Materials Science, Faculty of Science, Chiang Mai University, Chiang Mai 50200, Thailand*
[2] *Department of Chemistry, Faculty of Science, Chiang Mai University, Chiang Mai 50200, Thailand*
[3] *Materials Science Research Center, Faculty of Science, Chiang Mai University, Chiang Mai 50200, Thailand*

Correspondence should be addressed to Somchai Thongtem, schthongtem@yahoo.com

Received 1 October 2011; Accepted 8 November 2011

Academic Editor: William W. Yu

Orthorhombic α-MoO_3 microplates were produced from $(NH_4)_6Mo_7O_{24}\cdot 4H_2O$ solid powder by a 900 W microwave plasma for 40, 50, and 60 min. Phase, morphologies, and vibration modes were characterized by X-ray diffraction (XRD), selected area electron diffraction (SAED), scanning electron microscopy (SEM), and Raman and Fourier transform infrared (FTIR) spectroscopy. Sixty min processing resulted in the best crystallization of the α-MoO_3 phase, with photoluminescence (PL) in a wavelength range of 430–440 nm.

1. Introduction

Basically, molybdenum oxides are classified into two types: the thermodynamically stable orthorhombic α-MoO_3 phase, and the metastable monoclinic β-MoO_3 phase with ReO_3-type structure. Orthorhombic α-MoO_3 phase is a promising oxide, with structural anisotropy [1]. It is a wide bandgap n-type semiconductor, which is very attractive for different technological applications such as photochromic materials (changing from colorless to blue by UV irradiation) [2–4], smart windows [5], self-developing photography [2], conductive gas sensors [3], lubricants [6], and catalysts [7]. Orthorhombic α-MoO_3 was composed of MoO_6 octahedral corner-sharing chains, with edge sharing of two similar chains to form layers bonded by the weak van der Waals attraction [2]. Different methods were used to produce the oxide, which led to achieving products with different properties: evaporation of Mo foil by IR in 1 atm synthetic air to produce a uniformly semitransparent film on alumina substrate [3], direct oxidation of a Mo spiral coil in ambient atmosphere to produce film on Si (001) substrate [8], flash evaporation of molybdenum oxide powder on silica glass substrate, and (111)-oriented silicon wafer in vacuum [9], precipitation [10], and hydrothermal method [11].

In the present research, α-MoO_3 microplates were produced by exposing a solid powder to microwave plasma. This very simple and rapid process, which is also benign to the environment, may lead to large-scale industrial production.

2. Experiment

To produce MoO_3, $(NH_4)_6Mo_7O_{24}\cdot 4H_2O$ powder was used as a starting material without further purification. Each 0.5 g powder was loaded into three 14 mm I.D. $\times$ 100 mm long silica boats. Each was placed in a horizontal quart tube, which was tightly closed and evacuated until its absolute pressure was 3.7 ± 0.1 kPa. The powder was heated in batches by a 900 W microwave plasma; each batch was irradiated for 5 min. After the processing of each batch, the powder was thoroughly mixed and repeatedly heated for a total of 40, 50, or 60 min. During processing, the horizontal quart tube was continuously evacuated to drain the evolved gases out of the system.

The products were characterized using X-ray diffractometer (XRD, SIEMENS D500) operating at 20 kV, 15 mA, and

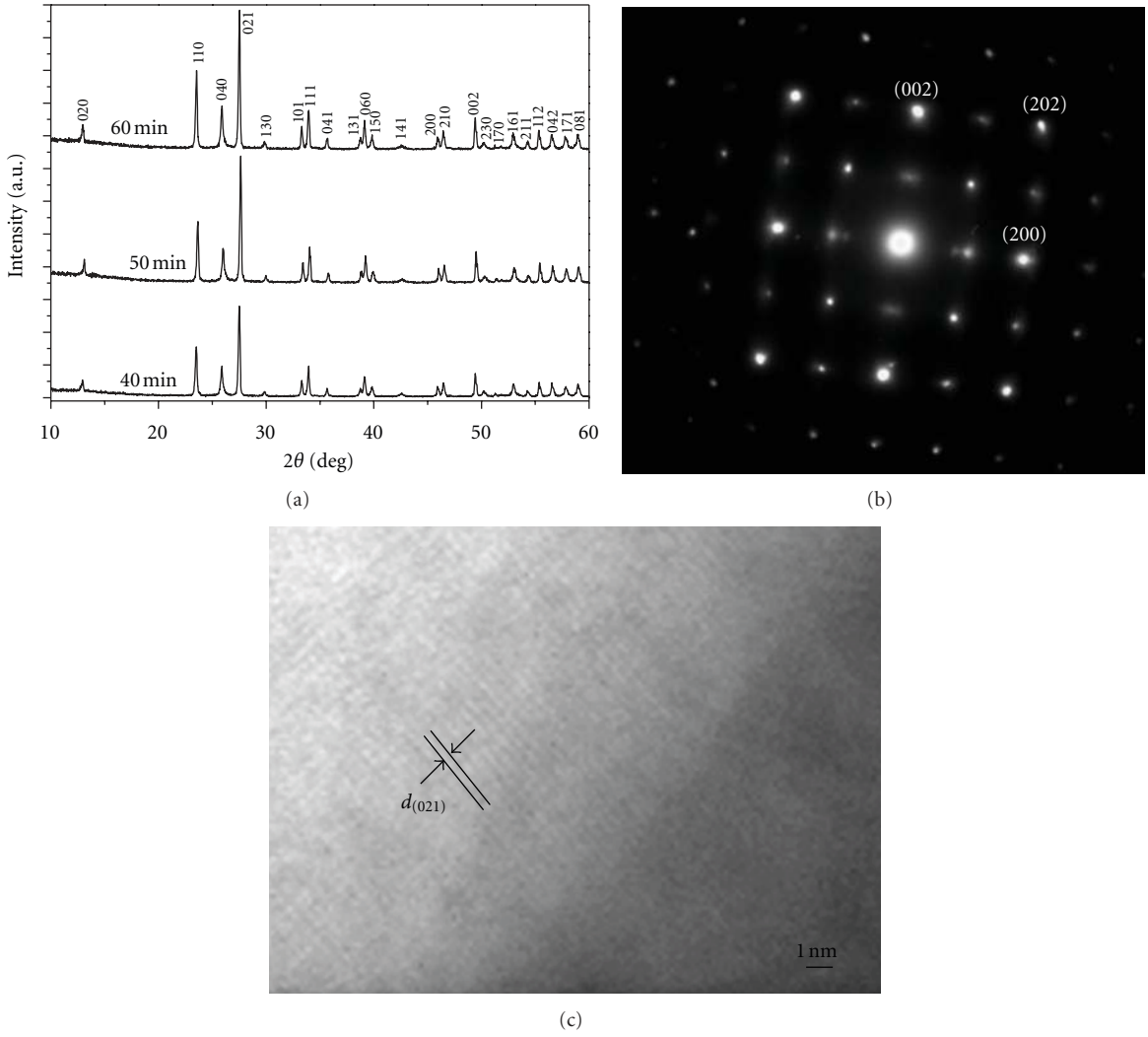

FIGURE 1: (a) XRD patterns of α-MoO_3 processed for 40, 50, and 60 min. (b, c) SAED pattern and HRTEM image of α-MoO_3 processed for 60 min.

using Cu-K_α line, in combination with the database of the Joint Committee on Powder Diffraction Standards (JCPDS) [12]; scanning electron microscope (SEM, JEOL JSM-6335F) operating at 15 kV, transmission electron microscope (TEM, JEOL JEM-2010), and selected area electron diffractometer (SAED) operating at 200 kV; Fourier transform infrared spectrometer (FTIR, Bruker Tensor 27) with KBr as a diluting agent and operated in the range of 2000–400 cm^{-1}, Raman spectrometer (T64000 HORIBA Jobin Yvon) using a 50 mW and 514.5 nm wavelength Ar green laser, and photoluminescence (PL) spectrometer (LS 50B PerkinElmer) using a 380 nm excitation wavelength at room temperature.

3. Results and Discussion

3.1. XRD, SAED, and HRTEM. XRD patterns of the products processed for 40, 50, and 60 min are shown in Figure 1(a). Their peaks were specified as orthorhombic MoO_3 of JCPDS database number 05–0508 [12], with no impurity detection. The (020) peaks at 2θ of 12.8° were clearly detected, and they indicated the presence of orthorhombic phase instead of monoclinic [13]. It should be noted that their intensities were slightly increased with the increase of processing time. The XRD peaks for 60 min processing time were the strongest, reflecting the product with the best degree of crystallinity. During processing, $(NH_4)_6Mo_7O_{24}\cdot 4H_2O$ decomposed as follows:

$$(NH_4)_6Mo_7O_{24}\cdot 4H_2O(s) \longrightarrow 7MoO_3(s) + 6NH_3(g) + 7H_2O(g) \quad (1)$$

$MoO_3(s)$ was left as the final solid products. Two gases (NH_3 and H_2O) diffused out of the system, and evacuated out of the horizontal quart tube. It should be noted that some reactant could remain, and was mixed with the final product if the processing time was less than 40 min. Longer processing times resulted in greater purification of the final product.

Calculated lattice parameters (Å) using the plane spacing equation for orthorhombic phase [14] were a = 3.96,

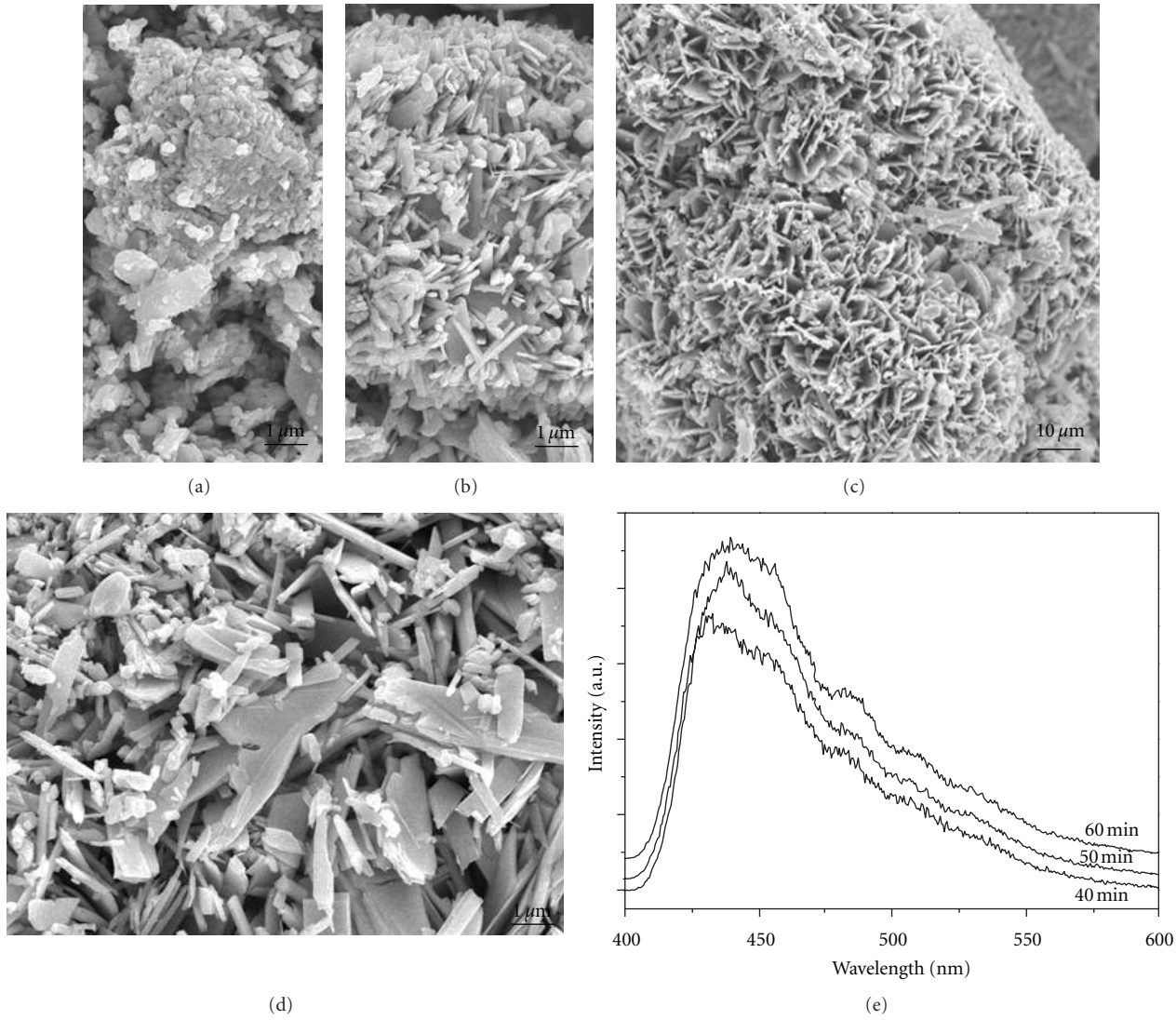

FIGURE 2: SEM images of α-MoO_3 processed for (a) 40 min, (b) 50 min, and (c, d) 60 min, and (e) PL emissions of α-MoO_3 processed for 40, 50, and 60 min.

b = 13.86, and c = 3.70, in accordance with those of the JCPDS database [12]. Figure 1(b) shows the SAED pattern of a single crystal processed for 60 min. It was indexed [15] to correspond with the (002), (202), and (200) crystallographic planes, which were specified as orthorhombic α-MoO_3 [2, 12, 16]. In the present analysis, an electron beam was sent to the crystal along the [010] direction. The (021) crystallographic plane with 0.33 nm spacing was detected by HRTEM (Figure 1(c)), implying that the product was crystalline in nature. These last two analyses were in accordance with that of the above XRD.

3.2. SEM. SEM images of MoO_3 crystals processed for 40, 50, and 60 min are shown in Figures 2(a)–2(d). Clusters of spheres ranging from 100 nm to a few hundred nm, as well as a small fraction of plates, were produced by 40 min processing. When the processing time was 50 min, more plates—about 100 nm thick and a few μm long—were produced, growing perpendicular to the cluster surface. Sixty min processing resulted in a further increase in the number of plates produced, as well as their sizes: 100–200 nm thick and a few μm long. During processing, some plates could be broken due to the internal stress developed inside.

3.3. Raman and FTIR Analyses. Raman spectra (Figure 3(a)) of MoO_3 crystals processed for 40, 50 and 60 min were studied in the range of 150–1050 cm^{-1}. During the analysis, a low-intensity laser was used to avoid crystallization. The product of 60 min processing was a highly ordered crystalline structure, and its Raman peaks were the highest. The heights were reduced when the processing time was shortened. In the present research, 12 typical Raman peaks were detected. The peaks at 990 cm^{-1} were specified as the Mo=O asymmetric stretching modes of terminal (unshared) oxygen [16]. The strongest peaks were at 813 cm^{-1}, and were specified as the doubly connected bridge-oxygen Mo_2–O stretching modes

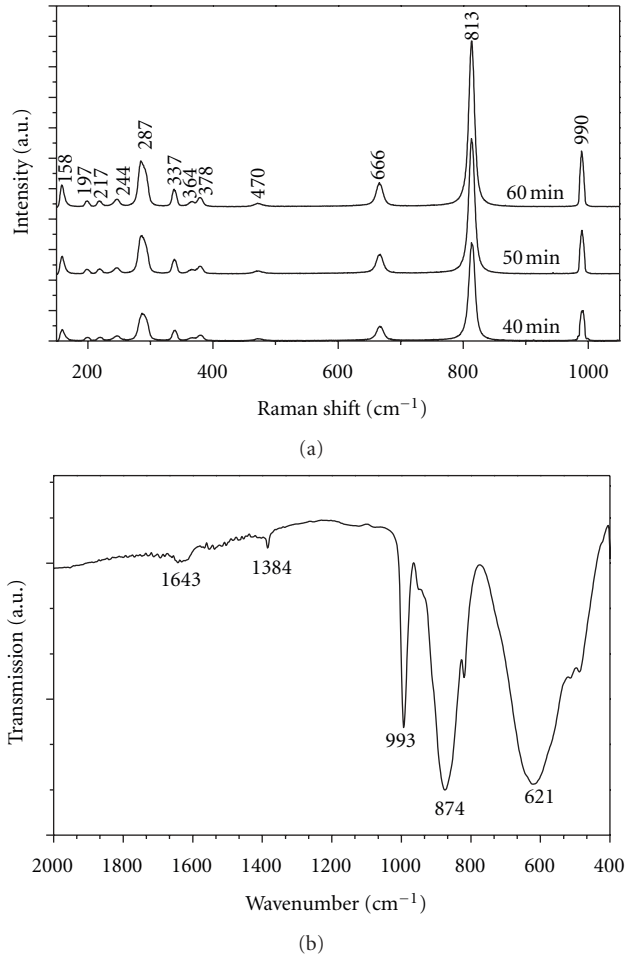

Figure 3: (a) Raman analysis of α-MoO_3 processed for 40, 50, and 60 min. (b) FTIR spectrum of α-MoO_3 processed for 60 min.

[2] of doubly coordinated oxygen, caused by corner-shared oxygen atoms in common to two MoO_6 octahedrons [16]. The peaks at 666 cm^{-1} were the Mo_3–O stretching modes of triply coordinated bridge-oxygen, caused by edge-shared oxygen atoms in common to three octahedrons [2, 16]. Their remains were the O–Mo–O asymmetric stretching/bending modes at 470 cm^{-1}, O–Mo–O scissoring modes at 378 and 364 cm^{-1}, O–Mo–O bending modes at 337 cm^{-1}, O=Mo=O wagging modes at 287 cm^{-1}, O=Mo=O twisting modes at 244 cm^{-1}, R_c modes at 217 cm^{-1}, O=Mo=O twisting modes at 197 cm^{-1}, and T_b modes at 158 cm^{-1} [16]. Sometimes the Raman peaks were positively/negatively shifted, due to the increase or decrease in the vibration constant of the products [2]. In the present research, the vibrations were the same values, although the processing time and degree of crystallinity were different.

Figure 3(b) shows the FTIR spectrum of α-MoO_3 over the 400–2000 cm^{-1} range. Three strong vibrations were detected at 621, 874 and 993 cm^{-1}, associated respectively with the stretching mode of oxygen linked with three metal atoms, the stretching mode of oxygen in the Mo–O–Mo units, and the Mo=O stretching mode—the specification of a layered orthorhombic α-MoO_3 phase [17]. Two weak vibrations were also detected at 1384 and 1643 cm^{-1}, associated with the vibration mode of the Mo–OH bond and the bending mode of adsorbed water, respectively [17, 18].

3.4. PL Emission. PL emission of orthorhombic α-MoO_3 processed for 40, 50, and 60 min was studied using 380 nm excitation wavelength at room temperature. The PL spectra (Figure 2(e)) presented broad peaks over the 400–600 nm range with a strong indigo emission centered at 430–440 nm—in accordance with the report of Song et al. [4]. These emissions were caused by the band-to-band transition. In the present research, very weak shoulders, caused by the electron-hole recombination between the conduction band and the sublevel of adsorbed oxygen acceptors, were also detected; these were able to be reduced by calcination at high temperatures [4]. The luminescence intensity increased with the increase of processing times, in accordance with the improvement of the degree of crystallinity characterized by the above XRD analysis.

4. Conclusions

Orthorhombic α-MoO_3 was successfully produced by a 900 W microwave plasma process for 40, 50, and 60 min. The product processed for 60 min was α-MoO_3 microplates with three main Raman peaks (666, 813, and 990 cm^{-1}), three main FTIR vibration modes (621, 874, and 993 cm^{-1}), and 430–440 nm indigo emission—a promising material for different applications.

Acknowledgments

The authors wish to thank the National Nanotechnology Center (NANOTEC), National Science and Technology Development Agency, Thailand, for providing financial support through the project code: P-10-11345, the Thailand's Office of the Higher Education Commission through the National Research University Project, and the Scholarships for Thai Ph.D. Program, and the Thailand Research Fund (TRF) through the TRF Research Grant, including the Graduate School of Chiang Mai University through the general support.

References

[1] X. W. Lou and H. C. Zeng, "Hydrothermal synthesis of α-MoO_3 nanorods via acidification of ammonium heptamolybdate tetrahydrate," *Chemistry of Materials*, vol. 14, no. 11, pp. 4781–4789, 2002.

[2] T. He and J. Yao, "Photochromism of molybdenum oxide," *Journal of Photochemistry and Photobiology C*, vol. 4, no. 2, pp. 125–143, 2003.

[3] E. Comini, L. Yubao, Y. Brando, and G. Sberveglieri, "Gas sensing properties of MoO_3 nanorods to CO and CH_3OH," *Chemical Physics Letters*, vol. 407, no. 4–6, pp. 368–371, 2005.

[4] J. Song, X. Ni, D. Zhang, and H. Zheng, "Fabrication and photoluminescence properties of hexagonal MoO_3 rods," *Solid State Sciences*, vol. 8, no. 10, pp. 1164–1167, 2006.

[5] T. He, Y. Ma, Y. Cao, Y. Yin, W. Yang, and J. Yao, "Enhanced visible-light coloration and its mechanism of MoO_3 thin films by Au nanoparticles," *Applied Surface Science*, vol. 180, no. 3-4, pp. 336–340, 2001.

[6] J. Wang, K. C. Rose, and C. M. Lieber, "Load-independent friction: MoO_3 nanocrystal lubricants," *The Journal of Physical Chemistry B*, vol. 103, no. 40, pp. 8405–8409, 1999.

[7] K. R. Reddy, K. Ramesh, K. K. Seela, V. V. Rao, and K. V. R. Chary, "Alkylation of phenol with methanol over molybdenum oxide supported on NaY zeolite," *Catalysis Communications*, vol. 4, no. 3, pp. 112–117, 2003.

[8] Y. Zhao, J. Liu, Y. Zhou et al., "Preparation of MoO_3 nanostructures and their optical properties," *Journal of Physics: Condensed Matter*, vol. 15, no. 35, pp. L547–L552, 2003.

[9] C. Julien, A. Khelfa, O. M. Hussain, and G. A. Nazri, "Synthesis and characterization of flash-evaporated MoO_3 thin films," *Journal of Crystal Growth*, vol. 156, no. 3, pp. 235–244, 1995.

[10] H. X. Bai, X. H. Liu, and Y. C. Zhang, "Synthesis of MoO_3 nanoplates from a metallorganic molecular precursor," *Materials Letters*, vol. 63, no. 1, pp. 100–102, 2009.

[11] T. Xia, Q. Li, X. Liu, J. Meng, and X. Cao, "Morphology-controllable synthesis and characterization of single-crystal molybdenum trioxide," *The Journal of Physical Chemistry B*, vol. 110, no. 5, pp. 2006–2012, 2006.

[12] Powder Diffract, File, JCPDS-ICDD, 12 Campus Boulevard, Newtown Square, P.A. 19073-3273, USA, 2001.

[13] T. Mizushima, K. Fukushima, H. Ohkita, and N. Kakuta, "Synthesis of β-MoO_3 through evaporation of HNO_3-added molybdic acid solution and its catalytic performance in partial oxidation of methanol," *Applied Catalysis A*, vol. 326, no. 1, pp. 106–112, 2007.

[14] C. Suryanarayana and M. G. Norton, *X-Ray Diffract*, Plenum Press, New York, USA, 1998.

[15] K. W. Andrews, D. J. Dyson, and S. R. Keown, *Interpretation of Electron Diffraction Patterns*, Plenum Press, New York, USA, 1971.

[16] T. Siciliano, A. Tepore, E. Filippo, G. Micocci, and M. Tepore, "Characteristics of molybdenum trioxide nanobelts prepared by thermal evaporation technique," *Materials Chemistry and Physics*, vol. 114, no. 2-3, pp. 687–691, 2009.

[17] G. S. Zakharova, C. Täschner, V. L. Volkov et al., "$MoO_{3-\delta}$ nanorods: synthesis, characterization and magnetic properties," *Solid State Sciences*, vol. 9, no. 11, pp. 1028–1032, 2007.

[18] M. Dhanasankar, K. K. Purushothaman, and G. Muralidharan, "Effect of temperature of annealing on optical, structural and electrochromic properties of sol-gel dip coated molybdenum oxide films," *Applied Surface Science*, vol. 257, no. 6, pp. 2074–2079, 2011.